DIFFUSION ACCELERATED DISCONTINUOUS FINITE ELEMENT SCHEMES FOR THE S_N EQUATIONS IN SLAB AND X,Y GEOMETRIES

Todd A. Wareing and Edward W. Larsen Department of Nuclear Engineering University of Michigan Ann Arbor, MI 48109

Marvin L. Adams
Lawrence Livermore National Laboratory
P.O. Box 808, L-18
Livermore, CA 94550

ABSTRACT

A new procedure is presented for diffusion-accelerating discontinuous finite element schemes for slab and x,y-geometry S_N problems. The novel feature of this procedure is that the discretized diffusion problem is derived from an asymptotic expansion of the discretized S_N problem. The motivation for this procedure is that the resulting diffusion problem is "simple" and easily solvable. Also, the asymptotic expansion shows that these discontinuous finite element schemes are highly accurate for diffusive problems with optically thick spatial meshes. Therefore, these schemes possess two highly desirable features: they are very accurate for optically thick spatial meshes, and they can be efficiently solved using diffusion synthetic acceleration.

I INTRODUCTION

Over the past two decades, a great deal of research has been directed toward accelerating the iterative convergence of S_N problems. Experience has shown that the Diffusion Synthetic Acceleration (DSA) method can be a very effective way to do this ^{1,2}. However, in two-dimensional geometries, only the diamond differenced S_N equations have been efficiently solved using DSA¹. This is because, for the 2-D diamond-differenced S_N equations, the standard DSA procedure leads to a relatively simple discretized low-order diffusion equation that for many problems can be efficiently solved by a multigrid method³. For other discretized versions of the S_N equations, using (for example) weighted diamond or linear discontinuous methods, the standard DSA procedure leads to much more complicated discretizations of the low-order diffusion equation that have not been efficiently solved by multigrid (or other) methods.

In this paper, we describe a new procedure to obtain discretized diffusion equations for DSA-accelerating the convergence of the S_N equations using certain lumped discontinuous finite element spatial differencing methods. The idea is to use an asymptotic analysis for the derivation of the discretized diffusion equation. This is based on the fact that diffusion theory is an asymptotic limit of transport theory.4

considered in this paper will be highly accurate for diffusive problems with spatial meshes that are very optically thick. Specifically, we apply this DSA procedure to a lumped Linear Discontinuous (LD) scheme for slab geometry and a lumped Bilinear Discontinuous (BLD) scheme for x,y-geometry.

A summary of the remainder of this paper follows. In Sec. II we describe the concept that underlies the DSA method. In Sec. III we describe the basic asymptotic relationship between transport and diffusion theory. We then derive and test our DSA method for slab geometry in Sec. IV, and for x,y-geometry in Sec. V. A brief discussion concludes the paper in Sec. VI.

II. BASICS OF DSA

Let us consider the standard SN equations in slab geometry with isotropic scattering:

$$\mu_m \frac{\partial}{\partial x} \psi_m(x) + \sigma_r(x) \psi_m(x) = \frac{\sigma_s(x)}{2} \phi(x) + \frac{Q(x)}{2} \quad , \tag{1}$$

$$\phi(x) = \sum_{m=1}^{N} \psi_m \mathbf{w}_m \tag{2}$$

The unaccelerated Source Iteration method for these equations is

$$\mu_{m} \frac{\partial}{\partial x} \psi_{m}^{(l+1/2)}(x) + \sigma_{t}(x) \psi_{m}^{(l+1/2)}(x) = \frac{\sigma_{s}(x)}{2} \phi^{(l)}(x) \quad , \tag{3}$$

$$\phi^{(l+1)}(x) = \sum_{m=1}^{N} \psi_m^{(l+1/2)} \mathbf{w}_m \tag{4}$$

This scheme converges slowly for optically thick problems with scattering ratios near unity. To accelerate convergence, we retain Eq. (3) but replace Eq. (4) by a more complicated, yet more efficient equation. To do this, we define a correction, f_{m} , such that

$$\psi_m(x) = \psi_m^{(l+1/2)}(x) + f_m(x) \tag{5}$$

Then, subtracting Eq (3) from Eq (1), we obtain

$$\mu_{m} \frac{\partial}{\partial x} f_{m}(x) + \sigma_{t}(x) f_{m}(x) - \frac{\sigma_{s}(x)}{2} \sum_{m=1}^{N} f_{m}(x) w_{m} = \frac{\sigma_{s}(x)}{2} \left(\phi^{(l+1/2)}(x) - \phi^{(l)}(x) \right)$$
 (6)

This equation for f_m is exact, but it is just as difficult to solve as the original equation Iherefore, for DSA, one approximates Eqs. (6) and (5) by the the diffusion approximation

$$-\frac{d}{dx}\frac{1}{3\sigma_{t}}\frac{d}{dx}f^{(l+1)}(x) + \sigma_{a}f^{(l+1)} = \sigma_{s}(\phi^{(l+1/2)}(x) - \phi^{(l)}(x)) \quad , \tag{7}$$

$$\phi^{(l+1)}(x) = \phi^{(l+1/2)}(x) + f^{(l+1)}(x)$$
(8)

Here $f^{(l+1)}$ is the diffusion approximation to f_m at the (l+1)-st iteration. To obtain a robust and efficient DSA procedure, the discretization of Eqs. (7) and (8) must be consistent with the discretization of Eqs. (3) and (5). To obtain the discretization for Eq. (7) we use the method of asymptotic expansions, and to obtain the discretization of Eq. (8) we use the standard DSA or P_1 method.

III ASYMPTOTIC DERIVATION OF THE LOW-ORDER DIFFUSION EQUATION

We assume that Eq. (6) is written in dimensionless form and invoke the assumptions for "diffusive" problems. That is, the physical medium is many mean free paths thick, and the cross sections, flux, and source are continuous and do not vary much over the distance of one mean free path. One obtains the following scaled S_N equations⁴:

$$\mu_{m} \frac{\partial}{\partial x} f_{m}(x) + \frac{\sigma_{t}(x)}{\varepsilon} f_{m}(x) - \frac{1}{2} \left(\frac{\sigma_{t}(x)}{\varepsilon} - \varepsilon \sigma_{a}(x) \right) \sum_{m=1}^{N} f_{m}(x) w_{m}$$

$$= \frac{\varepsilon \sigma_{s}}{2} \left(\phi^{(l+1/2)}(x) - \phi^{(l)}(x) \right)$$
(9)

Here ε depends on the particular characteristics of the transport problem. We see that for $\varepsilon = 1$, the problem remains unchanged, and for $\varepsilon << 1$, the problem is "diffusive." To determine the asymptotic solution of Eq. (9), we introduce the ansatz

$$f_m(x) \cong \sum_{k=0}^{\infty} \varepsilon^k f_{km}^{(l+1)}(x) \tag{10}$$

into Eq. (2) and equate the coefficients of ε^{-1} , ε^0 , and ε^1 . Then, recursively solving the resulting systems of equations, we obtain to leading order

$$f_m(x) = \frac{f_0^{(l+1)}(x)}{2} + O(\varepsilon)$$
 , (11)

where $f_0^{(l+1)}(x)$ solves the standard DSA diffusion equation

that

èen

Io

erefore,

(7)

(8)

$$-\frac{d}{dx}\frac{1}{3\sigma_{t}}\frac{d}{dx}f_{0}^{(l+1)}(x) + \sigma_{a}f_{0}^{(l+1)}(x) = \sigma_{s}\left(\phi^{(l+1/2)}(x) - \phi^{(l)}(x)\right)$$
 (12)

Thus, as $\varepsilon \to 0$, the solution of the continuous transport equation limits to the solution of the conventional diffusion equation. Certain discontinuous finite element schemes for the S_N equations have the property that when the same asymptotic analysis is applied to them on a fixed grid, one obtains an accurate discretized diffusion equation that can be solved efficiently by the multigrid method. We use these discretized S_N and diffusion equations in this paper.

We note that for a differencing scheme to possess this asymptotic limit is very significant, not only from the point of view of developing an efficient DSA procedure for it, but also from a point of view of accuracy⁴⁻⁶. This is because, in Eq. (9), as $\varepsilon \to 0$, the true transport cross section $\sigma_t(x)/\varepsilon$ tends to infinity, so the optical thickness of the spatial cells tends to infinity

11.1 2-3

Therefore, when a differencing scheme possesses this asymptotic limit, it means that there are diffusive problems for which the scheme will produce accurate results even for a very optically thick spatial grid. Most simple transport schemes, such as the diamond or weighted diamond schemes do not perform well for such problems.

IV. ASYMPTOTIC DSA METHOD FOR SLAB GEOMETRY

We have implemented this new "asymptotic" DSA procedure in slab geometry for the mass-lumped Linear-Discontinuous (LD) scheme⁵. The LD scheme with isotropic scattering is given by the following equations:

$$\frac{\mu_m}{\Delta x_i} (\psi_{m,j+1/2}^{(l+1/2)} - \psi_{m,j-1/2}^{(l+1/2)}) + \sigma_{t,j} \psi_{m,j}^{(l+1/2)} = \frac{1}{2} \left(\sigma_{s,j} \phi_j^{(l)} + Q_j \right) \quad , \tag{13a}$$

$$\frac{\theta_{m,j}\mu_m}{\Delta x_i} \left(\psi_{m,j+1/2}^{(l+1/2)} + \psi_{m,j-1/2}^{(l+1/2)} - 2\psi_{m,j} \right) + \sigma_{l,j} \hat{\psi}_{m,j}^{(l+1/2)} = \frac{1}{2} \left(\sigma_{s,j} \hat{\phi}_j^{(l)} + \hat{Q}_j \right) , \qquad (13b)$$

$$\psi_{m \ j \pm 1/2}^{(l+1/2)} = \psi_{m,j}^{(l+1/2)} \pm \hat{\psi}_{m,j}^{(l+1/2)} \qquad \mu_{m} \gtrsim 0 \tag{13c}$$

Here $\theta_{m,j} = 3$ for conventional LD and = 1 for the "mass-lumped" LD scheme. Experience has shown that conventional LD is more accurate for optically thin cells and "mass-lumped" LD is more accurate for optically thick cells. Interpolation between the two gives a modified LD scheme⁶ We use the "mass-lumped" $\theta_{m,j} = 1$ LD scheme in this analysis.

The LD equations for the correction $f_m^{(l+1)}$ are given by:

$$\frac{\mu_m}{\Delta x_i} \left(f_{m,j+1/2}^{(l+1)} - f_{m,j-1/2}^{(l+1)} \right) + \sigma_{t,j} f_{m,j}^{(l+1)} = \frac{\sigma_{s,j}}{2} \left(f_j^{(l+1)} + f_j^{(l+1/2)} \right) \quad , \tag{14a}$$

$$\frac{\mu_m}{\Delta x_j} \left(f_{m,j+1/2}^{(l+1)} + f_{m,j-1/2}^{(l+1)} - 2f_{m,j} \right) + \sigma_{t,j} \hat{f}_{m,j}^{(l+1)} = \frac{\sigma_{s,j}}{2} \left(\hat{f}_j^{(l+1)} + \hat{f}_j^{(l+1/2)} \right) \quad , \tag{14b}$$

$$f_{m,j\pm 1/2}^{(l+1)} = f_{m,j}^{(l+1)} \pm \hat{f}_{m,j}^{(l+1)} \quad \mu_m \ge 0$$
 , (14c)

where

$$f_i^{(l+1)} = \phi_i^{(l+1)} - \phi_i^{(l+1/2)} \quad , \tag{15a}$$

$$f_j^{(l+1/2)} = \phi_j^{(l+1/2)} - \phi_j^{(l)} \quad , \tag{15b}$$

$$\begin{split} f_{j}^{(l+1)} &= \phi_{j}^{(l+1)} - \phi_{j}^{(l+1/2)} &, \qquad (15a) \\ f_{j}^{(l+1/2)} &= \phi_{j}^{(l+1/2)} - \phi_{j}^{(l)} &, \qquad (15b) \\ \hat{f}_{j}^{(l+1)} &= \hat{\phi}_{j}^{(l+1)} - \hat{\phi}_{j}^{(l+1/2)} &, \qquad (15c) \\ \hat{f}_{j}^{(l+1/2)} &= \hat{\phi}_{j}^{(l+1/2)} - \hat{\phi}_{j}^{(l)} &. \qquad (15d) \end{split}$$

$$\hat{f}_{i}^{(l+1/2)} = \hat{\phi}_{i}^{(l+1/2)} - \hat{\phi}_{i}^{(l)} \tag{15d}$$

If we scale Eqs. (14) using the asymptotic scaling, we obtain the following:

$$\frac{\mu_{m}}{\Delta x_{j}} \left(f_{m,j+1/2}^{(l+1)} - f_{m,j-1/2}^{(l+1)} \right) + \frac{\sigma_{t,j}}{\varepsilon} f_{m,j}^{(l+1)} = \frac{1}{2} \left(\frac{\sigma_{t,j}}{\varepsilon} - \varepsilon \sigma_{a,j} \right) f_{j}^{(l+1)} + \frac{1}{2} \sigma_{s,j} f_{j}^{(l+1/2)} , \qquad (16a)$$

$$\frac{\mu_{m}}{\Delta x_{j}} \left(f_{m,j+1/2}^{(l+1)} + f_{m,j-1/2}^{(l+1)} - 2f_{m,j}^{(l+1)} \right) + \frac{\sigma_{t,j}}{\varepsilon} \hat{f}_{m,j}^{(l+1)} = \frac{1}{2} \left(\frac{\sigma_{t,j}}{\varepsilon} - \varepsilon \sigma_{a,j} \right) \hat{f}_{j}^{(l+1)} + \frac{1}{2} \sigma_{s,j} f_{j}^{(l+1/2)} , \quad (16b)$$

ptically iamond

$$f_{m,j\pm 1/2}^{(l+1)} = f_{m,j}^{(l+1)} \pm \hat{f}_{m,i}^{(l+1)} \qquad \mu_m \ge 0$$
 (16c)

Performing the same asymptotic analysis on these discretized equations as we performed on the continuous S_N equation, Eq. (9), we obtain for $\varepsilon \ll 1$

$$f_{m,j}^{(l+1)} = \frac{1}{4} \left(f_{j+1/2}^{(l+1)} + f_{j-1/2}^{(l+1)} \right) + O(\varepsilon) \quad , \tag{17}$$

where $f_{j+1/2}$ is the solution of the following diffusion equation, with a one point removal term:

$$-\frac{1}{3\sigma_{t,j+1}\Delta x_{j+1}} \left(f_{j+3/2}^{(l+1)} - f_{j+1/2}^{(l+1)}\right) + \frac{1}{3\sigma_{t,j}\Delta x_{j}} \left(f_{j+1/2}^{(l+1)} - f_{j-1/2}^{(l+1)}\right) + \frac{1}{2} \left(\sigma_{a,j+1}\Delta x_{j+1} + \sigma_{a,j}\Delta x_{j}\right) f_{j+1/2}^{(l+1)}$$

$$= \frac{1}{2} \left[\sigma_{s,j+1}\Delta x_{j+1} \left(f_{j+1}^{(l+1/2)} - \hat{f}_{j+1}^{(l+1/2)}\right) + \sigma_{s,j}\Delta x_{j} \left(f_{j}^{(l+1/2)} + \hat{f}_{j}^{(l+1/2)}\right)\right]$$
(18)

Now we devise a DSA method in which all the steps are the same as in the standard DSA method, except that Eq (18) is used instead of the standard diffusion equation derived by the P1 method [Boundary conditions for Eq. (18) are obtained from the P₁ approximation to Eqs. (14).] This gives us corrections to the scalar flux at the cell edges. We derive the "update" equations, which convert this information to cell-average scalar flux corrections, from the P1 approximation to Eqs. (14); these update equations are:

$$\phi_j^{(l+1)} = \phi_j^{(l+1/2)} + \frac{1}{\alpha_{1,j}} \left(\sigma_{s,j} f_j^{(l+1/2)} + \frac{\gamma_{1,j}}{2} (f_{j+1/2}^{(l+1)} + f_{j-1/2}^{(l+1)}) \right) , \qquad (19a)$$

$$\hat{\phi}_{j}^{(l+1)} = \hat{\phi}_{j}^{(l+1/2)} + \frac{1}{\alpha_{2,j}} \left(\sigma_{s,j} \hat{f}_{j}^{(l+1/2)} + \frac{\gamma_{2,j}}{2} (f_{j+1/2}^{(l+1)} - f_{j-1/2}^{(l+1)}) \right) , \qquad (19b)$$

where

$$\alpha_{1,j} = \frac{4}{3\sigma_{t,j}\Delta x_j^2} + \frac{2}{3\delta\Delta x_j} + \sigma_{a,j} \quad , \tag{20a}$$

$$\gamma_{1,j} = \alpha_{1,j} - \sigma_{a,j} \quad , \tag{20b}$$

$$\gamma_{1,j} = \alpha_{1,j} - \sigma_{a,j} , \qquad (20b)$$

$$\alpha_{2,j} = \frac{2\delta}{\Delta x_j} + \sigma_{a,j} , \qquad (21a)$$

$$\gamma_{2,j} = \alpha_{2,j} - \sigma_{a,j} \quad , \tag{21b}$$

and

$$\delta = \sum_{\mu_{-}>0} \mu_m \mathbf{w}_m \quad . \tag{22}$$

We have Fourier-analyzed and experimentally tested this scheme. Convergence results are given in Table 1; lack of space prevents us from exhibiting accuracy results, which are excellent For linearly anisotropic scattering with $0 < \overline{\mu} < 1$, the theoretical and experimental convergence results are nearly the same as those given in Table 1. We see that the "asymptotic" DSA procedure is very efficient, and that the theoretical and experimental results agree very closely Other calculations show that acceleration of the modified LD scheme is just as efficient as for the "lumped" scheme.

for the

ering is

164)

V. ASYMPTOTIC DSA METHOD FOR X,Y-GEOMETRY

For x,y-geometry, we use the Bilinear Discontinuous (BLD) finite element scheme with rectangular cells The Linear-Discontinuous (LD) finite element scheme does not result in a diffusion equation in the asymptotic limit⁶, so we cannot DSA-accelerate it We use a "lumped" BLD scheme proposed by Adams⁸ which, for uniform homogeneous cells, is given by:

$$\frac{\mu_m}{\Delta x} \left(\psi_{m\,i,+1/2\,\,j}^{(l+1/2)} - \psi_{m\,i,-1/2\,\,j}^{(l+1/2)} \right) + \frac{\eta_m}{\Delta y} \left(\psi_{m\,i,j+1/2}^{(l+1/2)} - \psi_{m\,i,j-1/2}^{(l+1/2)} \right) + \sigma_i \psi_{m\,i,j}^{(l+1/2)} = \sigma_s \phi_{i\,j}^{(l)} + Q_{i\,\,j} \;, \quad (23a)$$

$$\frac{\mu_{m}}{\Delta x} \left(\psi_{m,i+1/2,j}^{(l+1/2)} + \psi_{m,i-1/2,j}^{(l+1/2)} - 2 \psi_{m,i,j}^{(l+1/2)} \right) + \frac{\eta_{m}}{\Delta y} \left(\psi_{m,i,j+1/2}^{x,(l+1/2)} - \psi_{m,i,j-1/2}^{x,(l+1/2)} \right) \\
+ \sigma_{i} \psi_{m,i,j}^{x,(l+1/2)} = \sigma_{s} \phi_{i,i}^{x,(l)} + Q_{i,j}^{x} \quad , \tag{23b}$$

$$\begin{split} \frac{\mu_{m}}{\Delta x} \left(\psi_{m \ i+1/2 \ j}^{y,(l+1/2)} - \psi_{m \ i-1/2 \ j}^{y,(l+1/2)} \right) + \frac{\eta_{m}}{\Delta y} \left(\psi_{m \ i,j+1/2}^{(l+1/2)} + \psi_{m \ i,j-1/2}^{(l+1/2)} - 2 \psi_{m,i,j}^{(l+1/2)} \right) \\ + \sigma_{t} \psi_{m \ i,j}^{y,(l+1/2)} = \sigma_{s} \phi_{i \ j}^{y,(l)} + Q_{i,j}^{y} \quad , \end{split} \tag{23c}$$

$$\frac{\mu_m}{\Delta x} \left(\psi_{m\,i+1/2,j}^{y,(l+1/2)} + \psi_{m\,i-1/2,j}^{y,(l+1/2)} - 2\psi_{m\,i,j}^{y,(l+1/2)} \right) + \frac{\eta_m}{\Delta y} \left(\psi_{m\,i,j+1/2}^{x,(l+1/2)} + \psi_{m\,i,j-1/2}^{x,(l+1/2)} - 2\psi_{m\,i,j}^{x,(l+1/2)} \right)$$

$$+\sigma_{i}\psi_{m,i,j}^{xy,(l+1/2)} = \sigma_{s}\phi_{i,j}^{xy,(l)} + Q_{i,j}^{xy} \quad , \tag{23d}$$

$$\psi_{m,i\pm 1/2,j}^{(l+1/2)} = \psi_{m,i,j}^{(l+1/2)} \pm \psi_{m\,i,j}^{\times\,(l+1/2)} \quad \mu_m \gtrless 0 \quad , \tag{23e} \label{eq:23e}$$

$$\psi_{m \ i \pm 1/2, j}^{y, (l+1/2)} = \psi_{m \ i, j}^{y, (l+1/2)} \pm \psi_{m \ i, j}^{xy, (l+1/2)} \qquad \mu_{m} \ge 0 \quad , \tag{23}$$

$$\psi_{m\,i\,j\pm l/2}^{(l+1/2)} = \psi_{m\,i,j}^{(l+1/2)} \pm \psi_{m\,i,j}^{y,(l+1/2)} \qquad \eta_m \gtrless 0 \qquad , \tag{23g}$$

$$\psi_{m,i,j\pm1/2}^{\times(l+1/2)} = \psi_{m,i,j}^{\times(l+1/2)} \pm \psi_{m,i,j}^{\times(l+1/2)} \qquad \eta_{m} \ge 0$$
 (23h)

Following the same asymptotic procedure as in slab geometry, we obtain the following discretized diffusion equation for the correction factor used in the DSA procedure:

$$-\frac{1}{3\sigma_{t}\Delta x^{2}}\left[f_{i-1/2,j+1/2}^{(l+1)}-2f_{i+1/2,j+1/2}^{(l+1)}+f_{i+3/2,j+1/2}^{(l+1)}\right]$$

$$-\frac{1}{3\sigma_{t}\Delta y^{2}}\left[f_{i+1/2,j-1/2}^{(l+1)}-2f_{i+1/2,j+1/2}^{(l+1)}+f_{i+1/2,j+3/2}^{(l+1)}\right]+\frac{\sigma_{d}}{4}f_{i+1/2,j+1/2}^{(l+1)}$$

$$=\frac{\sigma_{s}}{4}\left[f_{i,j}^{(l+1/2)}+f_{i+1,j}^{(l+1/2)}+f_{i,j+1}^{(l+1/2)}+f_{i+1,j+1}^{(l+1/2)}+f_{i+1,j+1}^{(l+1/2)}+f_{i+1,j+1}^{(l+1/2)}+f_{i+1,j+1}^{(l+1/2)}-f_{i+1,j+1}^{s,(l+1/2)}-f_{i+1,j+1}^{s,(l+1/2)}-f_{i+1,j+1}^{s,(l+1/2)}-f_{i+1,j+1}^{s,(l+1/2)}+f_{i+1,j+1}^{sy,(l+1/2)}-f_{i+1,j}^{sy,(l+1/2)}-f_{i+1,j+1}^{sy,(l+1/2)}+f_{i+1,j+1}^{sy,(l+1/2)}-f_{i+1,j+1}^{sy,(l+1/2)}+f_{i+1,j+1}^{sy,(l+1/2)}\right]$$

$$(24)$$

in a

This gives corrections to the scalar flux at the cell vertices. [Boundary conditions for this equation are obtained from the P1 approximation to Eqs. (23)] The "update" equations, which convert this information to corrected cell-average scalar fluxes, are also derived using the P1 approximation to Eqs (23); these are:

$$\phi_{i,j}^{(l+1)} = \phi_{i,j}^{(l+1/2)} + \frac{1}{\alpha_1} \left[\sigma_s f_{i,j}^{(l+1/2)} + \frac{\gamma_1}{4} \begin{pmatrix} f_{i+1/2,j+1/2}^{(l+1)} + f_{i-1/2,j+1/2}^{(l+1)} \\ + f_{i+1/2,j-1/2}^{(l+1)} + f_{i-1/2,j-1/2}^{(l+1)} \end{pmatrix} \right] , \qquad (25a)$$

$$\phi_{i,j}^{x,(l+1)} = \phi_{i,j}^{x,(l+1/2)} + \frac{1}{\alpha_2} \left[\sigma_s f_{i,j}^{x,(l+1/2)} + \frac{\gamma_2}{4} \begin{pmatrix} f_{i+1/2,j+1/2}^{(l+1)} - f_{i-1/2,j+1/2}^{(l+1)} \\ + f_{i+1/2,j-1/2}^{(l+1)} - f_{i-1/2,j-1/2}^{(l+1)} \end{pmatrix} \right] , \quad (25b)$$

$$\phi_{i,j}^{\gamma,(l+1)} = \phi_{i,j}^{\gamma,(l+1/2)} + \frac{1}{\alpha_3} \begin{bmatrix} \sigma_s f_{i,j}^{\gamma,(l+1/2)} + \frac{\gamma_3}{4} \begin{pmatrix} f_{i+1/2,j-1/2}^{(l+1)} + f_{i-1/2,j-1/2}^{(l+1)} \\ -f_{i+1/2,j-1/2}^{(l+1)} - f_{i-1/2,j-1/2}^{(l+1)} \end{pmatrix} , \quad (25c)$$

$$\phi_{i,j}^{xy,(l+1)} = \phi_{i,j}^{xy,(l+1/2)} + \frac{1}{\alpha_4} \left[\sigma_s f_{i,j}^{xy,(l+1/2)} + \frac{\gamma_4}{4} \begin{pmatrix} f_{i+1/2,j+1/2}^{(l+1)} - f_{i-1/2,j+1/2}^{(l+1)} \\ -f_{i+1/2,j-1/2}^{(l+1)} + f_{i-1/2,j-1/2}^{(l+1)} \end{pmatrix} \right], \quad (25d)$$

where

$$\alpha_1 = \frac{4}{3\sigma_t} \left(\frac{1}{\Delta x^2} + \frac{1}{\Delta y^2} \right) + \frac{2}{3\delta} \left(\frac{1}{\Delta x} + \frac{1}{\Delta y} \right) + \sigma_a \quad , \tag{26a}$$

$$\gamma_1 = 2(\alpha_1 - \sigma_a) \quad , \tag{26b}$$

$$\alpha_2 = \frac{\gamma_1 = 2(\alpha_1 - \sigma_a)}{3\sigma_1 \Delta y^2} + \frac{2}{3\delta \Delta y} + \frac{2\delta}{\Delta x} + \sigma_a \quad , \tag{26b}$$

$$\gamma_2 = 2(\alpha_2 - \sigma_a) \quad , \tag{27b}$$

$$\gamma_2 = 2(\alpha_2 - \sigma_a) , \qquad (27b)$$

$$\alpha_3 = \frac{4}{3\sigma_t \Delta x^2} + \frac{2}{3\delta \Delta x} + \frac{2\delta}{\Delta y} + \sigma_a , \qquad (28a)$$

$$\gamma_3 = 2(\alpha_3 - \sigma_a) \quad , \tag{28b}$$

$$\alpha_4 = \frac{2\delta}{\Delta y} + \frac{2\delta}{\Delta x} + \sigma_a \quad , \tag{29a}$$

$$\gamma_4 = 2(\alpha_4 - \sigma_a) \quad , \tag{29b}$$

$$\gamma_4 = 2(\alpha_4 - \sigma_a) \quad , \tag{29b}$$

and

83

$$\delta = \sum_{\mu_m > 0} \mu_m \mathbf{w}_m = \sum_{\eta_m > 0} \eta_m \mathbf{w}_m \tag{30}$$

We have Fourier-analyzed and experimentally tested this scheme; convergence results are given in Tables 2 and 3. Table 2 gives the worst case results, for c = 1 and the S_4 quadrature set, and Table 3 gives the corresponding results for c = 0.95. In all cases shown in these tables, the agreement between theory (Fourier analysis) and experiment (the actual running of a code) is excellent. These results show that the 2-D version of the asymptotic DSA method will rapidly converge, provided that the aspect ratio of the cells in the spatial grid is not too large

Finally, we consider the heterogeneous 3-region, x,y-geometry problem with the configuration shown in Fig 1. We solved this problem with the S4 quadrature set and various uniform spatial grids, with a relative pointwise convergence criterion of 10-5 We calculated the

spectral radius, the leakage out the rightmost 2.0 cm on the top boundary, and the absorption rates in regions 1, 2, and 3; this data is all given in Table 4. For the coarsest mesh, the leakage result is not very accurate. However, the exact solution of this problem changes by about five orders of magnitude from the lower left corner of the system to the upper right corner, and in this crudest mesh, the numerical solution changes by an average amount of one order of magnitude across each cell. Therefore, this is an extremely crude mesh. All of the other numerical results are quite accurate, and in no case was a negative flux generated. Also, for all grids, the convergence of the DSA scheme is quite rapid. The most slowly converging grid required 14 iterations; the unaccelerated Source Iteration Scheme required about 100 iterations for this problem on each grid.

VI DISCUSSION

We have devised a new procedure for obtaining efficiently-solvable discretized diffusion equations that can be used in DSA calculations, and we have applied this procedure to lumped discontinuous finite-element methods in slab and x,y-geometries. Our procedure applies to discretized S_N schemes that produce, using an asymptotic expansion, a useful discretized diffusion equation. For a differencing scheme to have this asymptotic property is not just a mathematical curiosity; it implies that the scheme will be highly accurate in the diffusive S_N problems with very thick spatial meshes. Therefore, these schemes will have two very important properties: they will be highly accurate, and they will be efficiently and robustly solvable by a linear DSA procedure. Such schemes do not currently exist in production transport codes.

In future work, we plan to add anisotropic scattering to our x,y-geometry scheme and use DSA to accelerate the "current" as well as the "scalar flux" scattering terms; Morel has shown that this is essential in the numerical solution of charged particle transport problems. We also plan to implement the multigrid method for solving our low-order diffusion problem. Because this diffusion problem has a very simple 5-point stencil, it should be easy for readily-available multigrid solvers to solve it very efficiently. We also plan to examine acceleration methods for "modified" BLD problems, in which the lumping parameters are functions of the mesh width that interpolate between the unlumped BLD scheme for small meshes and the lumped scheme for large meshes. Finally, we plan to examine ways to improve the efficiency of our DSA scheme for x,y-geometry problems containing cells with large aspect ratios.

ACKNOWLEDGMENTS

Thework by the first two authors (I.A.W. and E.W.L.) was supported by NSF grant EEI-8721680 and Los Alamos National Laboratory. The early stages of this research were carried out during a summer internship by first author (T.A.W.) at LANL. Work of the third author (M.L.A.) was performed under the auspices of the U.S. Department of Energy by Lawrence Livermore National Laboratory under contract No. W-7405-Eng-48.

REFERENCES

1. R.E. Alcouffe, "Diffusion Synthetic Acceleration Methods for the Diamond-Differenced Discrete-Ordinates Equations", Nucl. Sci. Eng. 64, 344 (1977).

ption rates ge result is corders of his crudest cross each fis are quite ence of the ations; the reach grid

red diffusion e to lumped applies to red diffusion nathematical as with very les; they will A procedure.

heme and use as shown that also plan to because this ally-available methods for sh width that time for large heme for x,y-

NSF grant were carried third author Energy by

l-Differenced

- E.W. Larsen, "Unconditionally Stable Diffusion-Synthetic Acceleration Methods for the Slab Geometry Discrete-Ordinates Equations Part I: Theory", Nucl. Sci. Eng. 82, 47 (1982).
- 3. R.E. Alcouffe, A. Brandt, J.E. Dendy, and J. Painter, "The Multi-Grid Method for the Diffusion Equation with Strongly Discontinuous Coefficients", SIAM J. Sci. Comput. 2, 430 (1981).
- 4. E.W. Larsen, J.E. Morel, and W.F. Miller, Jr., "Asymptotic Solutions of Numerical Transport Problems in Optically Thick, Diffusive Regimes", J. Comp. Phys. 69, 283 (1987).
- 5 E.W. Larsen and J.E. Morel, "Asymptotic Solutions of Numerical Transport Problems in Optically Thick, Diffusive Regimes II", J. Comp. Phys. 83, 212 (1989).
- 6. C. Börgers, E.W. Larsen, and M.L. Adams, "The Asymptotic Diffusion Limit of a Linear Discontinuous Discretization of the Two-Dimensional Transport Calculation", J. Comp. Phys., to appear.
- 7 R. H. Szilard and G C Pomraning, "A Modified Linear Discontinuous Spatial Discretization Method in Planar Geometry", *Transp. Theory Stat. Phys.* 18, 255 (1989)
- M.L. Adams, "A New Transport Discretization Scheme for Arbitrary Spatial Meshes in X,Y-Geometry", these proceedings.
- 9 J.E. Morel, "A Synthetic Acceleration Method for Discrete Ordinates Calculations with Highly Anisotropic Scattering", Nucl Sci Eng 82, 34 (1982).

Table 1. Spectral Radius for Slab Geometry S16 LD Scheme With Isotropic Scattering

Δx (mfp)	Method	c = 0.5	c = 0.7	c = 09	c = 0.98
0.1	Theoretical	0.096	0.141	0.194	0 218
	Experimental	0.095	0.140	0.193	0 217
10	Theoretical	0 088	0 129	0.176	0.207
	Experimental	0 087	0 128	0.175	0.206
10.0	Theoretical	0.026	0.052	0.121	0.194
	Experimental	0.033	0.059	0.120	0.193
100.0	Theoretical	0.003	0 007	0.026	0.096
	Experimental	0.005	0.011	0.033	0.098

<u>Table 2. Spectral Radii for X.Y-Geometry S4 Lumped BLD Scheme</u>
<u>With Isotropic Scattering and c = 1.0</u>

Method	Δχ Δυ	0.5	1.0	5.0	10 0	20.0	40 0
Theoretical Experimental	0.5	0 342 0 328					
Theoretical Experimental	1.0	0 482 0 460	0.407 0.375				
Theoretical Experimental	5.0	0.820 0.773	0.784 0.749	0.531 0.514			
Theoretical Experimental	10.0	0.900 0.860	0.879 0.858	0.699 0.686	0.563 0.554		
Theoretical Experimental	20 0	0.947 0.910	0.935 0.920	0.825 0.816	0 718 0 711	0.591 0.579	
Theoretical Experimental	40.0	0.973 0.935	0.967 0.952	0 905 0 897	0 835 0 829	0.733 0.725	0 606 0 593

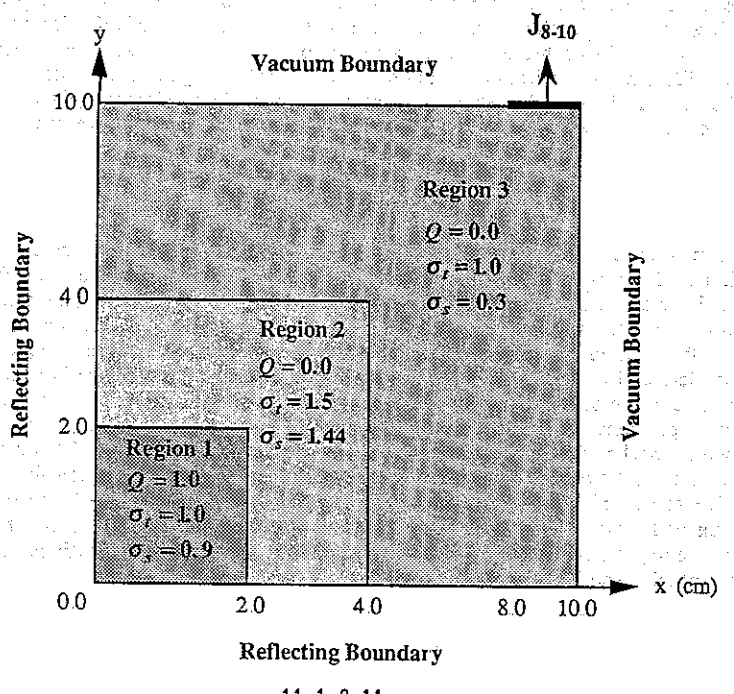
Table 3. Spectral Radii for X,Y-Geometry S₄ Lumped BLD Scheme With Isotropic Scattering and c=0.95

Method	Δχ Δυ	0.5	1.0	5.0	10 0	20.0	40.0
Theoretical Experimental	0.5	0.319 0.308					
Theoretical Experimental	1.0	0.456 0.434	0 381 0 368				
Theoretical Experimental	5.0	0 774 0 735	0.732 0.706	0 460 0 550			
Theoretical Experimental	10.0	0.850 0.813	0.820 0.800	0.593 0.580	0.457 0.447	:	
Theoretical Experimental	20.0	0.894 0.859	0.872 0.856	0.691 0.677	0.554 0.542	0.413 0.400	:
Theoretical Experimental	40.0	0:918 0.883	0 901 0 880	0.752 0.737	0.621 0.609	0.469 0.459	0.332 0.323

Table 4. Results for the X.Y-Geometry Heterogeneous Problem

Δx=Δy (cm)	Spectral Radius	J ₈₋₁₀	Abs. Rate Region 1	Abs. Rate Region 2	Abs. Rate Region 3
2.0	0 407	1 13x10 ⁻³	1.729	0.926	1.337
10	0.359	4.23x10 ⁻⁴	1.818	0 941	1 237
0.667	0.310	3.08x10 ⁻⁴	1 836	0.948	1.213
0.5	0.276	2.68x10 ⁻⁴	1 842	0.951	1 204
0.333	0.266	2.38x10 ⁻⁴	1.846	0.954	1 197

Figure 1 The X,Y-Geometry Heterogeneous Problem



11 .1 2-11

0:606 0:593

400 0.332 0.323